

A Method to Calculate the Spherical Multipole Expansion of the Electrostatic Charge Distribution on a Triangular Boundary Element

John Barrett^{1,*}, Joseph Formaggio¹, and Thomas Corona²

Abstract—We describe a technique to analytically compute the multipole moments of a charge distribution confined to a planar triangle, which may be useful in solving the Laplace equation using the fast multipole boundary element method (FMBEM) and for charged particle tracking. This algorithm proceeds by performing the necessary integration recursively within a specific coordinate system, and then transforming the moments into the global coordinate system through the application of rotation and translation operators. This method has been implemented and found use in conjunction with a simple piecewise constant collocation scheme, but is generalizable to non-uniform charge densities. When applied to low aspect ratio (≤ 100) triangles and expansions with degree up to 32, it is accurate and efficient compared to simple two-dimensional Gauss-Legendre quadrature.

1. INTRODUCTION

The behavior of systems under electrostatic forces is governed by the electric field \mathbf{E} , which can be expressed as the gradient of a scalar potential Φ :

$$\mathbf{E} = -\nabla\Phi. \quad (1)$$

In the absence of free charges, the potential Φ is determined by the Laplace equation,

$$\nabla^2\Phi = 0 \quad (2)$$

for all points \mathbf{x} in the simply connected domain Ω in \mathbb{R}^3 . The Laplace equation admits a unique solution for the field \mathbf{E} when the conditions on the boundary of the domain, $\partial\Omega$, are specified. The boundary conditions may be completely specified by associating either a value for the potential Φ (Dirichlet), or the derivative of Φ with respect to the surface normal $\frac{\partial\Phi}{\partial n}$ (Neumann), for every point on $\partial\Omega$.

One technique for numerically solving the Laplace equation is the boundary element method (BEM). Compared to other popular methods designed to accomplish the same goal, such as Finite Element and Finite Difference Methods [1], the BEM method focuses on the boundaries of the system rather than its domain, effectively reducing the dimensionality of the problem. BEM also facilitates the calculation of fields in regions that extend out to infinity (rather than restricting computation to a finite region) [2]. When it is applicable, these two features often make the BEM faster and more versatile than competing methods.

The basic underlying idea of the BEM involves reformulating the partial differential equation as a Fredholm integral equation of the first or second kind, defined respectively as,

$$f(\mathbf{x}) = \int_{\partial\Omega} K(\mathbf{x}, \mathbf{y})\Phi(\mathbf{y})d\mathbf{y} \quad (3)$$

Received 19 June 2015, Accepted 4 August 2015, Scheduled 12 August 2015

* Corresponding author: John Barrett (barrettj@mit.edu).

¹ Massachusetts Institute of Technology, Massachusetts, USA. ² University of North Carolina at Chapel Hill, North Carolina, USA.

and

$$\Phi(\mathbf{x}) = f(\mathbf{x}) + \lambda \int_{\partial\Omega} K(\mathbf{x}, \mathbf{y}) \Phi(\mathbf{y}) d\mathbf{y}, \quad (4)$$

where $K(\mathbf{x}, \mathbf{y})$ (known as the Fredholm kernel), and $f(\mathbf{x})$ are known, square-integrable functions, λ is a constant, and $\Phi(\mathbf{x})$ is the function for which a solution is sought. Discretizing the boundary of the domain into N elements and imposing the boundary conditions on this integral equation through either a collocation, Galerkin or Nyström scheme results in the formation of dense matrices which naively cost $\mathcal{O}(N^2)$ to compute and store and $\mathcal{O}(N^3)$ to solve [3]. This scaling makes solving large problems (much more than $\sim 10^4$ elements) impractical unless some underlying aspect of the equations involved can be exploited. For example, for the Laplace equation there exist iterative methods, such as Robin Hood [4, 5], which takes advantage of non-local charge transfer allowed by the elliptic nature of the equation to reduce the needed storage to $\mathcal{O}(N)$ and time of convergence to $\mathcal{O}(N^\alpha)$, with $1 < \alpha < 2$. Robin Hood solves the linear system by selectively modifying the charge distribution on the boundary element with the worst violation of the boundary conditions. After the modification, the residual is updated and the next boundary element to be modified is located. As such, it is a matrix-free method, but it requires a fast method to compute individual matrix elements, and unlike Krylov subspace methods, does not benefit from preconditioning techniques.

Another matrix-free technique that has been used to accelerate the BEM solution to the Laplace equation, that has also found wide applicability in three dimensional electrostatic, elastostatic, acoustic, and other problems, is the fast multipole method (FMM) [3]. The FMM was originally developed by V. Rokhlin and L. Greengard for the two dimensional Laplace boundary value problem [6] and N -body simulation [7]. Fast multipole methods are appropriate when the kernel of the equation is separable or approximately separable so that, to within some acceptable error, it may be expressed as a series [8],

$$K(\mathbf{x}, \mathbf{y}) \approx \sum_{k=0}^p \psi_k(\mathbf{x}) \xi_k(\mathbf{y}). \quad (5)$$

In the case of the Laplace equation, the kernel is often approximated by an expansion in spherical coordinates, with the functions $\psi_k(\mathbf{x})$ and $\xi_k(\mathbf{y})$ taking the form of the regular and irregular solid harmonics [9, 10]. This expansion allows the far-field effects of a source to be represented in a compressed form by a set of coefficients known as the *multipole moments* of the source. The series is truncated at a maximum degree of p which is determined by the desired precision.

When applying BEM together with FMM (which we refer to as FMBEM) to solve the Laplace equation over a complex geometry, it is necessary to determine the multipole moments of various subsets of the surfaces involved. At the smallest spatial scale, this requires a means of computing the individual multipole moments of each of the chosen basis functions (boundary elements). Geometrically, these basis functions usually take the form of planar triangular and rectangular elements, with the charge density on these elements either constant or interpolated between some set of sample points. Since rectangular elements cannot necessarily discretize an arbitrary curved surface without gaps or overlapping elements and can be decomposed into triangles, we consider it sufficient to compute the multipole expansion of basis functions of the triangular type.

Once the solution of the Laplace equation is known for a specific geometry and boundary conditions, a common task is to track charged particles throughout the resultant electrostatic field. Evaluating the field directly from all boundary elements of the geometry is costly. However, this process can be significantly accelerated by constructing a local or remote multipole expansion of the source field in the region of interest. The expansions can be precomputed with a time and memory cost which scales like $\mathcal{O}(Np^2)$, but result in field evaluation which scales like $\mathcal{O}(p^2)$, instead of $\mathcal{O}(N)$, as per the direct method. The usefulness of the multipole expansion in both FMBEM and charged particle tracking motivates us to find a method by which to compute the multipole expansion of a triangular boundary element accurately and efficiently.

2. MATHEMATICAL PRELIMINARIES

For an arbitrary collection of charges bounded within a sphere of radius R about the point \mathbf{x}_0 , there is a remote expansion for the potential $\Phi(\mathbf{x})$ given by [7, 11]:

$$\Phi(\mathbf{x}) = \sum_{l=0}^{\infty} \sum_{m=-l}^l \frac{Q_l^m Y_l^m(\theta, \phi)}{r^{l+1}}. \quad (6)$$

This approximation converges at all points \mathbf{x} such that $|\mathbf{x} - \mathbf{x}_0| > R$. The coefficients Q_l^m are known as the multipole moments of the charge distribution. The spherical harmonics $Y_l^m(\theta, \phi)$ are given by:

$$Y_l^m(\theta, \phi) = N_l^m P_l^{|m|}(\cos \theta) e^{im\phi}, \quad (7)$$

where the coordinates (r, θ, ϕ) are measured with respect to the origin \mathbf{x}_0 , and the function P_l^m is the associated Legendre polynomial of the first kind. Several normalization conventions exist for the spherical harmonics. Throughout this paper we use the Schmidt semi-normalized convention where $N_l^m = \sqrt{(l - |m|)! / (l + |m|)!}$. When the charge distribution $\sigma(\mathbf{x}')$ is confined to a surface Σ , the moments are given by the following integral:

$$Q_l^m = \int_{\Sigma} \sigma(\mathbf{x}) \overline{Y_l^m}(\theta, \phi) r^l d\Sigma = \int_{\Sigma} \sigma(\mathbf{x}) N_l^m P_l^{|m|}(\cos \theta) e^{-im\phi} r^l d\Sigma. \quad (8)$$

The integral given in Equation (8) can be addressed in a straightforward manner through two dimensional Gaussian quadrature [12]. It can also be reduced to a one dimensional Gaussian quadrature if one first computes an auxiliary vector field and applies Stokes' theorem, as described by Mousa et al. [13]. However, for high-order expansions, accurate evaluation of the numerical integration becomes progressively more expensive. It is therefore desirable to obtain an analytic expression of the multipole moments.

3. COORDINATE SYSTEM FOR INTEGRATION

In order to compute the multipole expansion of a triangle Σ defined by points $\{\mathbf{P}_0, \mathbf{P}_1, \mathbf{P}_2\}$ in the global coordinate system S'' , we first must select the appropriate local coordinate system to simplify the integration. Without loss of generality, we choose a system so that the vertex \mathbf{P}_0 lies at the origin, and the $\hat{\mathbf{e}}_1$ direction is parallel to the vector $\mathbf{P}_2 - \mathbf{P}_1$. The plane defined by the triangle is then parameterized by the local coordinates (u, v) . Formally, this local coordinate system S can be defined with the following origin and basis vectors:

$$S : \begin{cases} \mathcal{O} = \mathbf{P}_0 \\ \hat{\mathbf{e}}_0 = \frac{\mathbf{Q} - \mathbf{P}_0}{|\mathbf{Q} - \mathbf{P}_0|} \\ \hat{\mathbf{e}}_1 = \frac{\mathbf{P}_2 - \mathbf{P}_1}{|\mathbf{P}_2 - \mathbf{P}_1|} \\ \hat{\mathbf{e}}_2 = \hat{\mathbf{e}}_0 \times \hat{\mathbf{e}}_1 \end{cases}. \quad (9)$$

The point \mathbf{Q} is the closest point to \mathbf{P}_0 lying on the line joining \mathbf{P}_1 and \mathbf{P}_2 . The position of \mathbf{Q} in the (u, v) -plane is $(h, 0)$ and is given by $\mathbf{Q} = \mathbf{P}_1 + ((\mathbf{P}_0 - \mathbf{P}_1) \cdot \hat{\mathbf{e}}_1) \hat{\mathbf{e}}_1$. Figure 1 shows the arrangement of the two coordinate systems.

4. EVALUATION BY RECURRENCE

For an arbitrary expansion origin and surface element, Equation (8) is very difficult to compute analytically, even for a constant charge density. Additionally, the variety of schemes available for function interpolation over triangular domains, such as the natural orthogonal polynomial basis put forth in [14–17], or the more commonly used variations on Lagrange and Hermite interpolation [18–21],

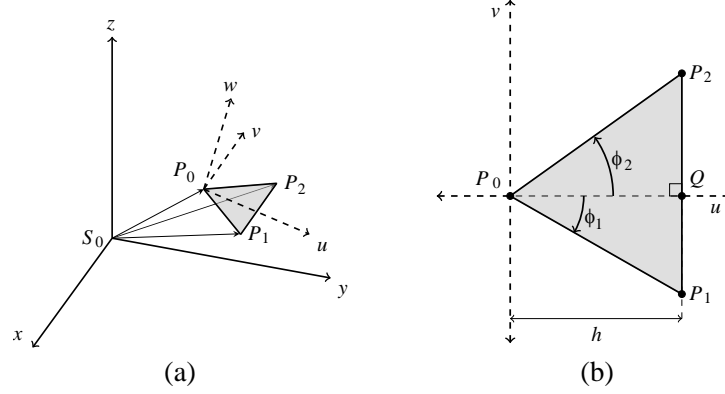


Figure 1. The boundary element Σ (shaded region) in global and local coordinate systems. (a) Triangle Σ with arbitrary orientation and position in global coordinate system S'' . (b) Triangle Σ in local coordinate system S used for integration (w axis points out of the page).

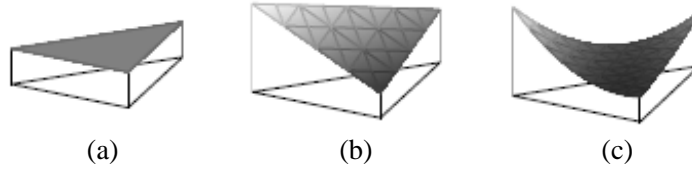


Figure 2. Planar boundary elements with various orders of charge density interpolation. Height above the element indicates the value of the local charge density. (a) Zero-th order, $N = 0$. (b) First order, $N = 1$. (c) Second order, $N = 2$.

complicates any general approach. Therefore in order to proceed, we choose a simplifying restriction on the general problem, and avoid these more advanced interpolation schemes in favor of a simpler but less well-conditioned bivariate monomial basis. In this basis, the charge density on the triangle is expressed in terms of local orthogonal coordinates (u, v) by:

$$\sigma(u, v) = \begin{cases} \sum_{a=0}^N \sum_{b=0}^{N-a} s_{a,b} u^a v^b & : (u, v) \in \Sigma \\ 0 & : (u, v) \notin \Sigma \end{cases} \quad (10)$$

where N is the order of the interpolation, the variables (u, v) are as defined in Figure 1, and $s_{a,b}$ are the interpolation coefficients. Figure 2 shows an example of the interpolated function for various N . It is possible to perform a change of basis on the interpolating polynomials [22] to compute the $s_{a,b}$ coefficients in terms of the coefficients of some other polynomial basis, however we will defer discussion of this change of basis and its application to low-order Lagrange interpolation to Appendix B.

It is convenient to perform the integral in the spherical coordinate system associated with S , since the (u, v) -plane is a surface of constant θ where the differential surface element $d\Sigma = r \sin \theta dr d\phi$. Since the local coordinates (u, v) are

$$u(r, \phi) = r \cos \phi \quad (11)$$

$$v(r, \phi) = r \sin \phi, \quad (12)$$

the expression for the charge density becomes:

$$\sigma(r, \phi) = \begin{cases} \sum_{a=0}^N \sum_{b=0}^{N-a} s_{a,b} (r \cos \phi)^a (r \sin \phi)^b & : (r, \phi) \in \Sigma \\ 0 & : (r, \phi) \notin \Sigma \end{cases} \quad (13)$$

Fixing $\theta = \pi/2$, inserting our expression for the charge density (13) into (8) and then exchanging the

order of integration and summation we find:

$$Q_l^m = \sum_{a=0}^N \sum_{b=0}^{N-a} s_{a,b} N_l^m P_l^{|m|}(0) \int_{\phi_1}^{\phi_2} \int_0^{r(\phi)} (\cos \phi)^a (\sin \phi)^b e^{-im\phi} r^{a+b+l+1} dr d\phi. \quad (14)$$

As can be seen in Figure 1 the upper limit on the r integration is given by $r(\phi) = h/\cos \phi$. Performing the integration over the r coordinate leaves us with:

$$Q_l^m = \sum_{a=0}^N \sum_{b=0}^{N-a} \underbrace{\left(\frac{s_{a,b} h^{a+b+l+2}}{a+b+l+2} \right) N_l^m P_l^m(0)}_{\mathcal{K}_{l,m}^{a,b}} \underbrace{\int_{\phi_1}^{\phi_2} \frac{(\sin \phi)^b e^{-im\phi}}{(\cos \phi)^{b+l+2}} d\phi}_{\mathcal{I}_{l,m}^b}. \quad (15)$$

The prefactors $\mathcal{K}_{l,m}^{a,b}$ are easy to compute. To address integrals of the form $\mathcal{I}_{l,m}^b$ we split our integrand into imaginary and real components $\mathcal{I}_{l,m}^b = \mathcal{A}_{l,m}^b - i\mathcal{B}_{l,m}^b$, where

$$\mathcal{A}_{l,m}^b = \int_{\phi_1}^{\phi_2} \frac{(\sin \phi)^b \cos(m\phi)}{(\cos \phi)^{b+l+2}} d\phi \quad (16)$$

$$\mathcal{B}_{l,m}^b = \int_{\phi_1}^{\phi_2} \frac{(\sin \phi)^b \sin(m\phi)}{(\cos \phi)^{b+l+2}} d\phi. \quad (17)$$

Before evaluating these integrals, we pause to introduce the Chebyshev polynomials [23, 24]. The Chebyshev polynomials of the first kind $T_n(x)$ are defined recursively for $n \geq 0$ through:

$$T_{n+1}(x) = 2xT_n(x) - T_{n-1}(x), \quad (18)$$

with $T_0(x) = 1$ and $T_1(x) = x$. Similarly, the Chebyshev polynomials of the second kind, $U_n(x)$, are defined through:

$$U_{n+1}(x) = 2xU_n(x) - U_{n-1}(x), \quad (19)$$

with $U_0(x) = 1$ and $U_1(x) = 2x$. These polynomials are noteworthy for our purposes because of the two following useful properties:

$$T_n(\cos \phi) = \cos(n\phi) \quad (20)$$

$$U_n(\cos \phi) = \frac{\sin((n+1)\phi)}{\sin \phi}. \quad (21)$$

We can exploit these in order to evaluate $\mathcal{A}_{l,m}^b$ and $\mathcal{B}_{l,m}^b$ recursively. We first address $\mathcal{A}_{l,m}^b$. Using (20), we may rewrite (16) as

$$\mathcal{A}_{l,m}^b = \int_{\phi_1}^{\phi_2} \frac{(\sin \phi)^b T_m(\cos \phi)}{(\cos \phi)^{b+l+2}} d\phi. \quad (22)$$

Expanding this using (18) gives

$$\mathcal{A}_{l,m}^b = 2 \int_{\phi_1}^{\phi_2} \frac{(\sin \phi)^b T_{m-1}(\cos \phi)}{(\cos \phi)^{b+l+1}} d\phi - \int_{\phi_1}^{\phi_2} \frac{(\sin \phi)^b T_{m-2}(\cos \phi)}{(\cos \phi)^{b+l+2}} d\phi, \quad (23)$$

which yields the recursion relationship for the $\mathcal{A}_{l,m}^b$:

$$\mathcal{A}_{l,m}^b = 2\mathcal{A}_{l-1,m-1}^b - \mathcal{A}_{l,m-2}^b. \quad (24)$$

Similarly for the $\mathcal{B}_{l,m}^b$, we have:

$$\mathcal{B}_{l,m}^b = 2\mathcal{B}_{l-1,m-1}^b - \mathcal{B}_{l,m-2}^b. \quad (25)$$

Given these recursion relationships, we can reduce the integrals $\mathcal{A}_{l,m}^b$ and $\mathcal{B}_{l,m}^b$ of any degree $0 \leq l$ and order $0 \leq m \leq l$ into a series of terms, of which only the base cases must be evaluated explicitly.

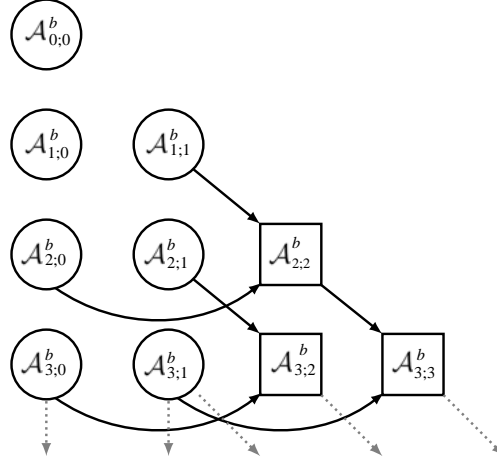


Figure 3. Graphical representation of recursion given in Equation (24) up to $l = 3$. Circles denote terms which must be computed as a base case, squares denote terms which may be computed by recurrence. The arrows indicate dependence. Higher order terms extend downwards and to the right, as denoted by the dotted lines and arrows.

Figure 3 shows a representation of the recursion relationship. The base cases that are not further reducible through recurrence can all be expressed in terms of single integral form I_p^q where

$$I_p^q = \int_{\phi_1}^{\phi_2} \frac{(\sin \phi)^q}{(\cos \phi)^p} d\phi. \quad (26)$$

The base cases $\mathcal{A}_{l,0}^b = I_{b+l+2}^b$ and $\mathcal{A}_{l,1}^b = I_{b+l+1}^b$, while $\mathcal{B}_{l,1}^b = I_{b+l+2}^{b+1}$ and $\mathcal{B}_{l,0}^b = 0$. The solutions to integrals of the form I_p^q are addressed in Appendix A.

It should be noted that during the process of computing the value of the moment Q_l^m through recursion, the real and imaginary parts of all moments with degree $\leq l$ and order $\leq m$ will be computed. These values can be stored so that there is no need to repeat the recursion for each individual moment needed. This is useful when determining the multipole expansion of a boundary element since all moments up to a certain maximal degree can be computed in one pass through the recurrence.

5. MULTIPOLE MOMENTS UNDER COORDINATE TRANSFORMATION

We can make use of the results of the preceding section to compute the multipole expansion coefficients of the boundary element Σ with respect to an arbitrary origin and set of coordinate axes. Typically, we are most interested in being able to construct the multipole moments q_l^m of Σ in the coordinate system that has the canonical Cartesian coordinate axes, with an origin at an arbitrary point \mathbf{S}_0 . We refer to this system as the global coordinate system, and denote it as S'' :

$$S'' : \begin{cases} \mathcal{O} = \mathbf{S}_0 \\ \hat{e}_0'' = (1, 0, 0) \\ \hat{e}_1'' = (0, 1, 0) \\ \hat{e}_2'' = (0, 0, 1) \end{cases}. \quad (27)$$

Therefore, we must first construct the coordinate transformation $A : S \rightarrow S''$, and then determine how this coordinate transform operates on the coefficients Q_l^m of the multipole expansion given in S . The rigid motion $A : S \rightarrow S''$ can be specified by a rotation $U : S \rightarrow S'$ followed by a translation $T : S' \rightarrow S''$. We can describe the translation by the displacement $\Delta = \mathbf{S}_0 - \mathbf{P}_0$, and the rotation U by the Euler angles (α, β, γ) following the $Z - Y' - Z''$ axis convention of [25, 26]. The Euler angles allow us to write the rotation U as the composition of three successive rotations $U = U_{Z''}(\gamma)U_{Y'}(\beta)U_Z(\alpha)$.

Table 1. Euler angles in terms of the elements of the matrix U .

Angle	$U_{22} \neq \pm 1$	$U_{22} = 1$	$U_{22} = -1$
α	$\text{atan2}(\frac{-U_{21}}{\sin \beta}, \frac{-U_{20}}{\sin \beta})$	0	π
β	$\text{acos}(U_{22})$	$\text{atan2}(U_{10}, U_{00})$	$\text{atan2}(U_{01}, U_{11})$
γ	$\text{atan2}(\frac{-U_{12}}{\sin \beta}, \frac{-U_{02}}{\sin \beta})$	0	0

Explicitly, U is given by

$$U = \begin{bmatrix} \cos \gamma & -\sin \gamma & 0 \\ \sin \gamma & \cos \gamma & 0 \\ 0 & 0 & 1 \end{bmatrix} \begin{bmatrix} \cos \beta & 0 & -\sin \beta \\ 0 & 1 & 0 \\ \sin \beta & 0 & \cos \beta \end{bmatrix} \begin{bmatrix} \cos \alpha & -\sin \alpha & 0 \\ \sin \alpha & \cos \alpha & 0 \\ 0 & 0 & 1 \end{bmatrix} \quad (28)$$

and can be related to the basis vectors of the coordinate system S by:

$$U = \begin{bmatrix} U_{00} & U_{01} & U_{02} \\ U_{10} & U_{11} & U_{12} \\ U_{20} & U_{21} & U_{22} \end{bmatrix} = \begin{bmatrix} \hat{e}_0 \\ \hat{e}_1 \\ \hat{e}_2 \end{bmatrix}^T. \quad (29)$$

It is well known that the Euler angles (α, β, γ) do not uniquely describe an arbitrary rotation matrix U , however, a unique description is not necessary for our purposes. A convenient set of choices is given in Table 1. With the transformation $A : S \rightarrow S''$ specified by the Euler angles (α, β, γ) and the displacement Δ , we can determine the multipole moments of Σ in S'' through the application of theorems (1) and (2).

Theorem (1), from Wigner [27], originates in quantum mechanics [28]. It appears when needing to express the result of the action of the rotation operator $\mathcal{D}^l(\alpha, \beta, \gamma)$ upon a particular eigenstate $|l, m\rangle$ of total angular momentum l , which is associated with the spherical harmonic $Y_l^m(\theta, \phi)$, in terms of the eigenstates of the rotated frame $|l', m'\rangle$. Note that since total angular momentum is conserved, this rotation operator does not mix states with a distinct value of l (thus $l = l'$). Specifically, Wigner's theorem tells us the matrix elements of the rotation operator $\mathcal{D}^l(\alpha, \beta, \gamma)$, which is a member of the $(2l + 1) \times (2l + 1)$ matrix representation of $SO(3)^\dagger$. A more succinct version of this theorem is given in [26], and is restated here in slightly a modified form.

Theorem 1 Assume there are two coordinate systems which share the same origin $S : (\mathcal{O}, \hat{e}_0, \hat{e}_1, \hat{e}_2)$ and $S' : (\mathcal{O}, \hat{e}'_0, \hat{e}'_1, \hat{e}'_2)$, that are related by the rotation $U \in SO(3)$ specified by the Euler angles $\{\alpha, \beta, \gamma\}$ such that $\hat{e}'_i = U\hat{e}_i$, for $i = 0, 1, 2$. Furthermore assume that there is a function $F(\theta, \phi)$ that can be expanded in terms of the spherical harmonics $Y_l^m(\theta, \phi)$ such that:

$$F(\theta, \phi) = \sum_{l=0}^{\infty} \sum_{m=-l}^l Q_l^m Y_l^m(\theta, \phi) \quad (30)$$

then there exists a function $f(\theta', \phi')$ such that:

$$f(\theta', \phi') = F(\theta(\theta', \phi'), \phi(\theta', \phi')) = \sum_{l=0}^{\infty} \sum_{m'=-l}^l q_l^{m'} Y_l^{m'}(\theta', \phi') \quad (31)$$

where the coefficients $q_l^{m'}$ are given by:

$$q_l^{m'} = \sum_{m=-l}^l \mathcal{D}_{m',m}^l(\alpha, \beta, \gamma) Q_l^m \quad (32)$$

and where $\mathcal{D}_{m',m}^l(\alpha, \beta, \gamma)$ are elements of what is know as the Wigner D -matrix.

[†] The special orthogonal group $SO(3)$ is the group of all 3×3 orthogonal matrices under matrix multiplication. It is an irreducible representation of the rotation group, which is the set of all rotations about the origin in \mathbb{R}^3 under the operation of composition.

The direct evaluation of the coefficients $\mathcal{D}_{m',m}^l(\alpha, \beta, \gamma)$ through the use of the expressions given by Wigner [27, 28] is beyond the scope of this paper. Regardless, direct evaluation of (32) is known to be inefficient, as well as numerically unstable for large values of l and certain angles [29]. However, given the wide applicability of spherical harmonics to quantum chemistry, fast multipole methods, and other areas, there has recently been a large effort to develop efficient and stable methods to perform such rotations in both real and complex spherical harmonic bases. The current state of the field of spherical harmonic rotation is well summarized by [30], with the algorithm developed by Pinchon et al. [25] being one of the fastest and most accurate. To avoid the need of complex matrix-vector multiplication, the method proposed by Pinchon et al. [25] is executed in the basis of real spherical harmonics $S_l^m(\theta, \phi)$ (with a different normalization convention). To apply a rotation to the set of multipole moments $\{Q_l^m\}$, with l fixed and m ranging from $-l$ to l , we first must calculate the corresponding real basis $\{R_l^m\}$ coefficients. Then, to prepare this set of moments $\{R_l^m\}$ for the rotation operator we arrange them to form the column vector \mathbf{R}_l :

$$\mathbf{R}_l = \left[R_l^{-l}, R_l^{-l+1}, R_l^{-l+2}, \dots, R_l^{l-1}, R_l^l \right]^T. \quad (33)$$

The application of the Wigner \mathcal{D}^l -matrix to this column vector produces the corresponding vector of rotated moments \mathbf{r}_l . For efficiency, the \mathcal{D}^l -matrix is itself decomposed into several matrices, each of which may be applied to the vector \mathbf{R}_l in succession:

$$\mathbf{r}_l = \mathcal{D}^l(\alpha, \beta, \gamma)\mathbf{R}_l = [X_l(\alpha)J_lX_l(\beta)J_lX_l(\gamma)]\mathbf{R}_l. \quad (34)$$

In this notation, the X_l matrices effect a rotation about the z -axis, while the J_l matrices perform an interchange of the y and z axes. The advantage to this method is that the X_l matrices have a simple sparse form whose action on the vector \mathbf{R}_l can be computed quickly, as they consist only of non-zero diagonal and anti-diagonal terms. The interchange matrices J_l , on the other hand, are completely independent of the rotation angles and therefore only need to be computed once. While the computation of J_l is beyond the scope of this paper, there is an elegant recursive scheme to compute them up to any degree l given by Pinchon et al. [25]. After the rotated moments \mathbf{r}_l have been computed in the real basis, we need only convert them back to the complex basis to obtain the set of moments $\{q_l^{m'}\}$.

After obtaining the multipole moments $\{q_l^{m'}\}$ in the coordinate system S' , we need to determine how they are modified by a displacement of the expansion origin. This can be accomplished by the application of theorem (2). This theorem, presented by Greengard and Rokhlin [6, 7], is a principle part of the fast multipole method. It is applied during the operation of gathering the multipole expansions of smaller regions into larger collections, and describes how a multipole expansion about one origin can be re-expressed as an expansion about a different origin. Graphically, this is represented in Figure 4.

Theorem 2 *Consider a multipole expansion with coefficients $\{O_n^m\}$ due to charges located within the sphere D with radius a centered about the point \mathbf{P}_0 . This expansion converges for points outside of sphere D . Now consider the point $\mathbf{S}_0 \notin D$ such that $\Delta = \mathbf{S}_0 - \mathbf{P}_0 = (\rho, \alpha, \beta)$. We may form a new multipole expansion about the point \mathbf{S}_0 due to the charges within D which converges for points outside of the sphere D' that has its center at \mathbf{S}_0 and radius $a' = \rho + a$. The multipole moments of the new expansion $\{M_j^k\}$ are given by:*

$$M_j^k = \sum_{n=0}^j \sum_{m=-n}^{m=n} \frac{O_{j-n}^{k-m} i^{|k|-|m|-|k-m|} A_n^m A_{j-n}^{k-m} \rho^n Y_n^{-m}(\alpha, \beta)}{A_j^k} \quad (35)$$

where $A_n^m = (-1)^n / \sqrt{(n-m)!(n+m)!}$.

Applying theorem (2), with the displacement $\Delta = \mathbf{S}_0 - \mathbf{P}_0$ and the rotated moments $\{q_l^{m'}\}$ inserted as $\{O_n^m\}$ allows us to obtain the set of moments $\{M_j^k\}$ which are equivalent to the final objective, namely, the multipole moments $\{q_l^m\}$ of the boundary element Σ in the global coordinate system S'' . However, the number of arithmetic operations required by the application of theorem (2) scales like $\mathcal{O}(p^4)$. This high cost can be mitigated by the use of the special case of theorem (2) along the z -axis. White et al. [31] noted that it can be used to perform a multipole-to-multipole translation along any axis needed if a

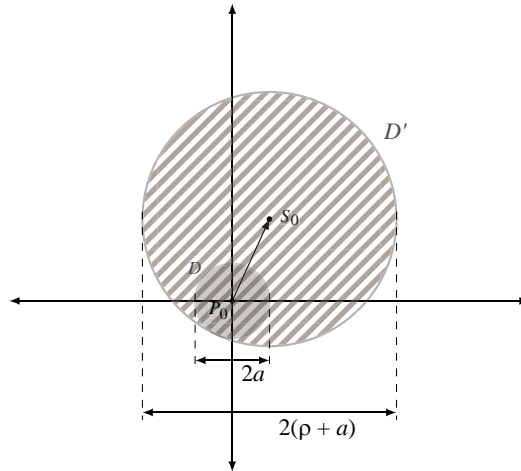


Figure 4. Multipole to multipole translation. The solid shaded area indicates the region where the original multipole expansion $\{O_n^m\}$ does not converge, the striped area indicates the region where the new multipole expansion $\{M_j^k\}$ does not converge.

rotation is performed through the use of theorem (1) before and after the translation operation. The first rotation applied aligns the z -axis with the vector $\mathbf{S}_0 - \mathbf{P}_0$, while the second rotation is the inverse. The use of the rotation operator together with the axial translation has a cost which scales like $\mathcal{O}(p^3)$, which for high-degree expansions can provide useful acceleration when compared to the implementation of theorem (2) alone.

Using theorem (2) to transform the multipole moments computed about the expansion center \mathbf{P}_0 (in the special coordinate system S), to an arbitrary expansion center \mathbf{S}_0 puts a constraint on the radius of convergence. The radius of convergence can be no less than $\rho + a$, where $\rho = |\mathbf{P}_0 - \mathbf{S}_0|$ and a is the length of the longest side of the triangle Σ that terminates on \mathbf{P}_0 .

6. NUMERICAL RESULTS

In order to gain some understanding of the accuracy and efficiency of the algorithm presented in this work, some numerical tests were performed with regard to the problem of evaluating the electrostatic potential of a uniformly charged triangle (zero-th order interpolant). All of the following tests were performed in double precision.

Since the integrals required to compute the multipole expansion of boundary elements are typically evaluated using numerical quadrature, a straightforward two dimensional Gauss-Legendre quadrature method was used as a benchmark against which to compare the speed and accuracy of the analytic algorithm. It should be noted that this numerical integration routine has not been optimized, nor is it the most efficient possible, it is only intended to provide a point of reference to a typically used means of computing the multipole coefficients. There are several techniques to accelerate the numerical integration over our benchmark implementation, such as adaptive quadrature [32] or quadrature rules specifically formulated for triangular domains such as those of Cowper [33]. Cowper's rules require roughly three times fewer function evaluations than the two-dimension Gauss-Legendre with corresponding accuracy but are only provided for a few different orders. The computation of the weights and abscissa for an arbitrary order quadrature rule on a triangular domain is more complicated than the simple two-dimensional scheme, which are trivially generated from the one dimensional Gauss-Legendre weights and abscissa. Though it is possible that these other methods may be competitive, they were not implemented for this study, since it is not the purpose of this paper to survey the broad range of numerical integration methods available.

The benchmark numerical integration is performed by first converting the integral over the triangular domain given by the points $\{\mathbf{P}_0, \mathbf{P}_1, \mathbf{P}_2\}$ to an integral over a rectangular domain through the use of a slightly modified version of the transform described by Duffy [34]. We can then write the

surface integral given in Equation (8) as:

$$Q_l^m = \int_0^{L_1} \int_0^{L_2} \sigma_0 \overline{Y}_l^m(\theta(\mathbf{r}), \phi(\mathbf{r})) |\mathbf{r}|^l \left| \frac{\partial \mathbf{r}}{\partial u} \times \frac{\partial \mathbf{r}}{\partial v} \right| dv du = \int_0^{L_1} \int_0^{L_2} f(u, v) dv du, \quad (36)$$

where $\mathbf{r}(u, v) = (\mathbf{P}_0 + u\hat{\mathbf{n}}_1 + v(1 - u/L_1)\hat{\mathbf{n}}_2) - \mathbf{x}_0$. The point \mathbf{x}_0 is the origin of the expansion, $L_i = |\mathbf{P}_i - \mathbf{P}_0|$, and $\hat{\mathbf{n}}_i = (\mathbf{P}_i - \mathbf{P}_0)/L_i$ for $i = 1, 2$. The two dimensional integral over the (u, v) -plane is then performed using m -th order two dimensional Gauss-Legendre quadrature [23], given by:

$$Q_l^m = \frac{L_1 L_2}{4} \sum_{i=1}^m \sum_{j=1}^m w_i w_j f\left(\frac{L_1}{2}(x_i + 1), \frac{L_2}{2}(x_j + 1)\right) \quad (37)$$

where w_i and x_i are respectively, the one-dimensional Gauss-Legendre weights and abscissa as described by Golub and Welsch [35].

The first study consisted of 10^4 triangles generated by randomly selecting points on a sphere with arbitrary radius R_{source} . These triangles were restricted to have an aspect ratio of less than 100. We define the aspect ratio of a triangle as the base divided by the height, with the base taken to be the longest side. For each triangle the multipole expansion (for each degree up to $p = 32$) about the origin \mathbf{x}_0 (the center of the sphere) was calculated using the algorithm described in this work. For each triangle 100 random points \mathbf{x} were selected in the volume $R_{\text{source}} < |\mathbf{x} - \mathbf{x}_0| < 10^3 \times R_{\text{source}}$. The angular coordinates of these points were uniformly distributed, while the radial coordinate followed a log uniform distribution in order to provide enough statistics for points at small radius. At each test point the relative error between the potential evaluated directly and the potential given by the multipole expansion was computed and histogrammed. The relative error $\Phi_{\text{error}} = |(\Phi_{\text{multipole}} - \Phi_{\text{direct}})/\Phi_{\text{direct}}|$ on the potential is plotted as a function relative distance from the expansion origin for various expansion degrees in Figure 5. The relative error on a $p = 32$ degree expansion of the potential reaches approximately machine precision at roughly twice R_{source} . However, the constraint imposed by theorem (2) on the radius of convergence in this particular test geometry limits the minimum radius of convergence to approximately $2 \times R_{\text{source}}$. Using a higher degree expansion than 32 does not result in a reduced radius of convergence for this geometry.

As a general rule, Φ_{error} is a decreasing function of distance until numerical roundoff starts to dominate near the level of machine precision. However, this is only true so long as the method used

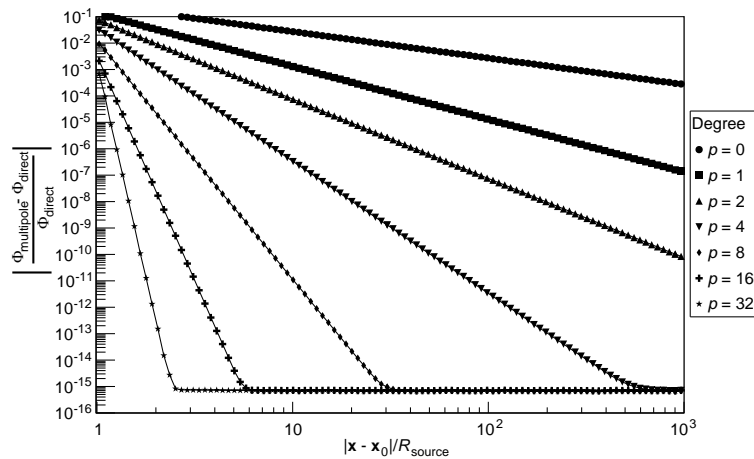


Figure 5. Comparison of the accuracy of the multipole expansion against the direct method of evaluating the potential with various degrees of the expansion. Coefficients of the multipole expansion are calculated using the analytic method described in this paper. Relative error is shown as a function of the ratio $|\mathbf{x} - \mathbf{x}_0|/R_{\text{source}}$, where $|\mathbf{x} - \mathbf{x}_0|$ is the distance of the evaluation point from the expansion origin, and R_{source} is the radius of the smallest sphere enclosing the charge distribution.

to compute the multipole moments of the expansion respects the oscillatory behavior of the spherical harmonics. For low degree expansions, numerical quadrature rules with a small number of function evaluations can compute the multipole moments exactly to within machine precision. However, as the degree of the expansion is increased the higher order spherical harmonics oscillate more rapidly and progressively more expensive quadrature rules are needed to evaluate the coefficients to equivalent accuracy. To explore this effect we repeated the previous study using our algorithm and the benchmark numerical quadrature method with various orders $m = \{2, 3, 4, 6, 8, 10\}$ and defined a quantity $R_{\text{convergence}}$ (the radius of convergence) as the minimum distance $|\mathbf{x} - \mathbf{x}_0|$ for which we have $\Phi_{\text{error}}(\mathbf{x})$ less than some threshold t_{error} . Then for each method and expansion degree up to $p = 32$ we computed the radius of convergence at four thresholds $t_{\text{error}} = \{10^{-5}, 10^{-8}, 10^{-11}, 10^{-14}\}$. Figure 6 shows the behavior of $R_{\text{convergence}}/R_{\text{source}}$ as a function of expansion degree. For example, from Figure 6 one can see that up to an expansion degree of $p = 8$, the 4×4 Gauss-Legendre quadrature rule is sufficient to compute the multipole coefficients to the same accuracy as our algorithm. However continuing to use the 4×4 Gauss-Legendre quadrature rule while increasing the degree of the expansion up to $p = 32$ does not result in a more accurate evaluation of the potential. To obtain the full benefit of a high degree expansion one must correspondingly increase the number of function evaluations used by numerical integration.

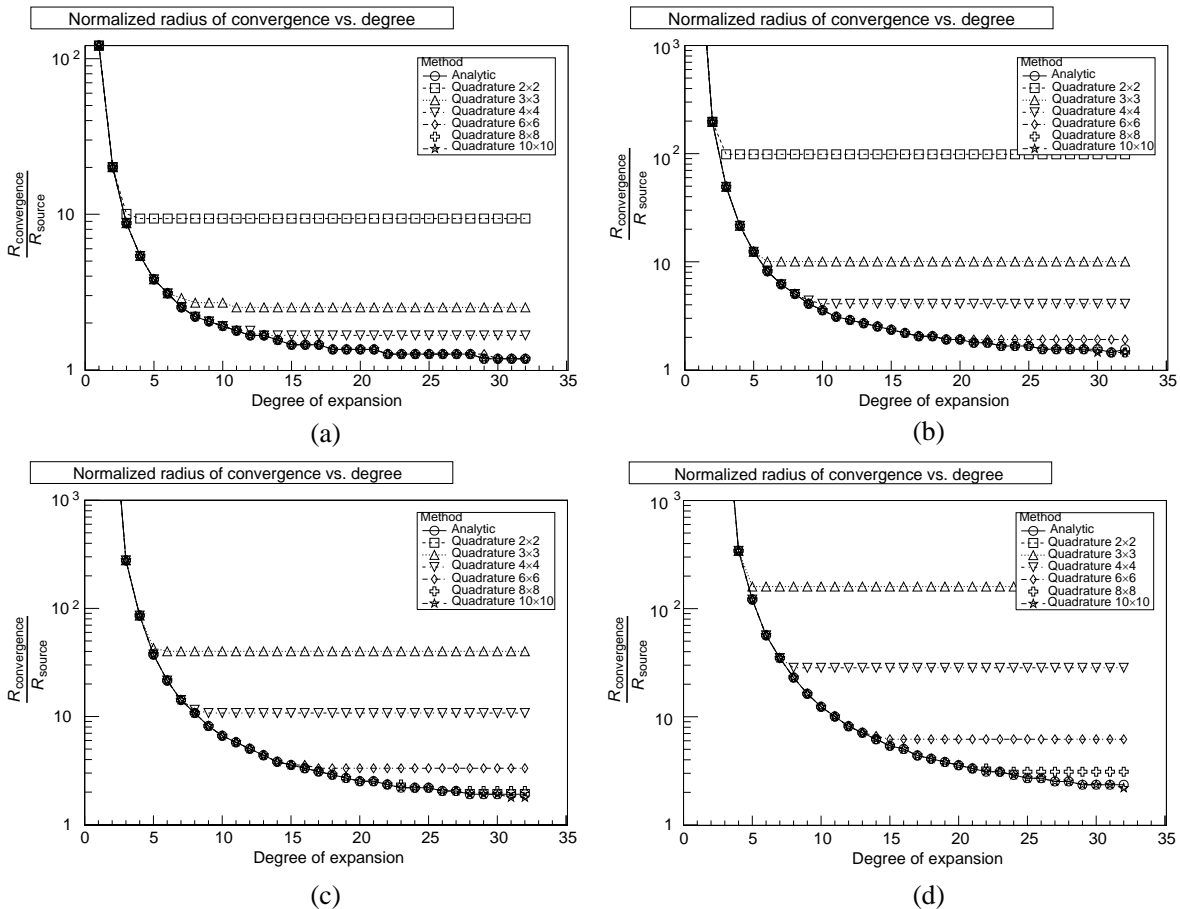


Figure 6. Relative radius of convergence as a function of the degree of the multipole expansion for various thresholds on the relative error and different methods of calculating the multipole moments. For quadrature rules which compute the multipole moments with insufficient accuracy the radius of convergence fails to decrease after reaching a certain degree. Note that up to $p = 32$ the 10×10 Gauss-Legendre quadrature rule computes the multipole moments to equivalent accuracy as algorithm (1). (a) Threshold of 10^{-5} . (b) Threshold of 10^{-8} . (c) Threshold of 10^{-11} . (d) Threshold of 10^{-14} .

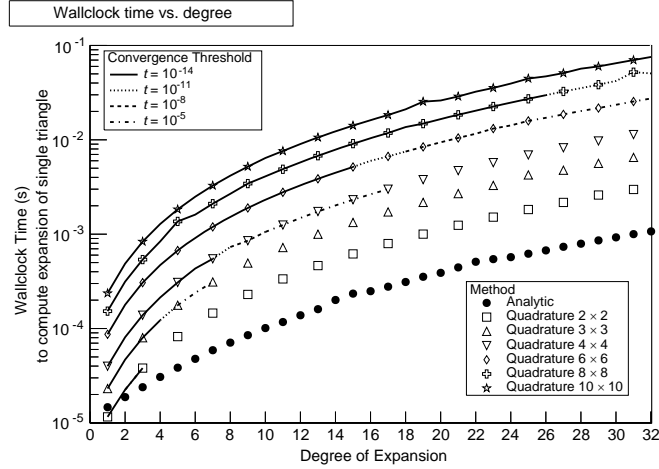


Figure 7. Wallclock time required to evaluate all of the multipole coefficients of a single triangle for the method detailed in algorithm (1) and various $m \times m$ point Gauss-Legendre quadrature. In order to make a direct comparison between the several methods it is necessary to fix an upper limit t_{error} on the allowed relative error of the potential computed from the multipole coefficients of the triangle. The spherical volume of space where the relative error is everywhere less than t_{error} has a radius defined as the radius of convergence $R_{\text{convergence}}$. If the radius of convergence associated with any $m \times m$ quadrature rule is $\leq 1.2 \times R_{\text{convergence}}$ of the analytic method then we say it has roughly equivalent accuracy and draw a line through the corresponding point on the timing graph. The line style denotes the value of t_{error} used when defining the radius of convergence. If its radius of convergence is larger, then that particular quadrature rule has failed to meet the same accuracy as the analytic method and no line is drawn. For example, for $t_{\text{error}} = 10^{-14}$ the 4×4 quadrature rule and the analytic method are both satisfactory up to $p = 7$, however, above $p = 17$ the 4×4 rule does not compute the multipole coefficients as accurately as the analytic method even if the required threshold t_{error} is set as low as 10^{-5} .

To demonstrate the efficiency of this algorithm (at least in regard to the naive two dimensional numerical integration using Gauss-Legendre quadrature), a comparison was made between the time needed to compute all of the multipole expansion coefficients of a single triangle (up to a certain degree) using the analytic algorithm and the time needed when using numerical integration. This test was carried out on a computer with an Intel i7 processor running at 1.9 GHz, results are shown in Figure 7. Individually the scaling of all methods is $\mathcal{O}(p^2)$ since this is approximately the number of moments to be computed. However, beyond a certain maximal degree, a fixed order numerical quadrature rule will no longer compute the multipole moments to a given threshold t_{error} , and a higher order rule will be needed to retain accuracy making the scaling of numerical integration effectively greater than $\mathcal{O}(p^2)$. This difference in scaling can be seen Figure 7 by noting how the position of the end of the solid line (cut off for $t_{\text{error}} = 10^{-14}$) has a larger slope than the analytic method. For all but the lowest degree $p \leq 4$ expansions, the performance of the algorithm presented in this work is approximately an order of magnitude faster than the lowest accuracy Gauss-Legendre quadrature rule considered, while for the highest degree tested ($p = 32$) it is nearly two orders of magnitude faster than the quadrature rule which obtains equivalent accuracy.

Finally, to demonstrate the usage of this method in solving the Laplace equation with FMBEM, we solved a simple unit cube capacitor with Dirichlet boundary conditions with several choices for the number of boundary elements and the expansion order p . The results are shown in Figure 8. To solve the linear system the Krylov method GMRES [36] was used, with the iterative solver being terminated when the relative L_2 norm of the residual was less than 10^{-8} . The error on the unit cube capacitance was taken to be the relative difference between the calculated value and the value given by Read [37], which is $0.6606785 \pm 6 \times 10^{-7}$ (in units of $4\pi\epsilon_0$).

Unfortunately, the analytic method of computing the multipole moments is not applicable in all cases. The first restriction is that the aspect ratio of the triangle must not be too large (exceeding 100).

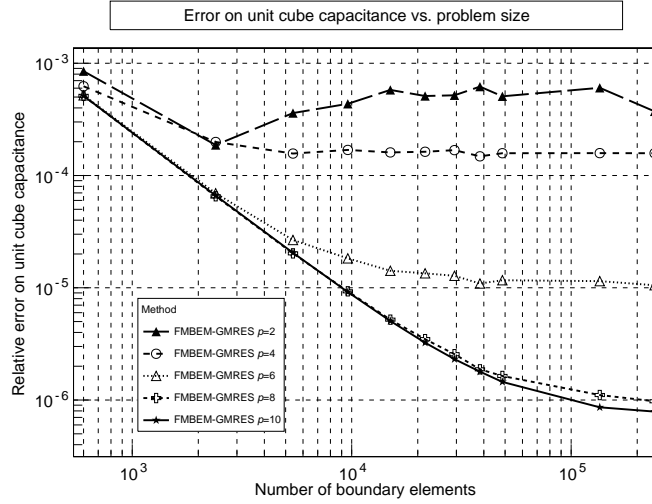


Figure 8. Accuracy of unit cube capacitance computed by FMBEM for various discretization scales and expansion degree. Algorithm (1) was used to compute the multipole moments of the boundary elements used by the FMBEM. Note that for a large number of boundary elements and high expansion degree, the error on the FMBEM calculated capacitance approaches the error on value given by the reference [37].

Algorithm 1 Computing the multipole moments of a triangular boundary element.

Input: Triangle $\Sigma : \{\mathbf{P}_0, \mathbf{P}_1, \mathbf{P}_2\}$ and associated charge density interpolation coefficients $\{s_{ab}\}$.

- 1: Compute height h and coordinate system S for triangle Σ according to Equation (9).
- 2: **for** $l = 0$ to p **do**
- 3: **for** $m = 0$ to l **do**
- 4: **for all** $s_{a,b} \neq 0$ **do**
- 5: Compute the prefactor $\mathcal{K}_{l,m}^{a,b}$ according to Equation (15).
- 6: Recursively compute the integral $\mathcal{I}_{l,m}^b$ according to Equations (24) and (25).
- 7: **end for**
- 8: Compute the multipole moment $Q_l^m = \sum_a \sum_b \mathcal{K}_{l,m}^{a,b} \mathcal{I}_{l,m}^b$ and $Q_l^{-m} = \overline{Q_l^m}$.
- 9: **end for**
- 10: **end for**
- 11: Compute the Euler angles (α, β, γ) of the rotation $U : S \rightarrow S'$ according to Table 1.
- 12: Apply the rotation U on the set of moments; $\{Q_l^m\} \rightarrow \{q_l^{m'}\}$ using theorem (1).
- 13: Apply the translation $\Delta : S' \rightarrow S''$ on the moments; $\{q_l^{m'}\} \rightarrow \{q_l^m\}$ using theorem (2).

Output: The multipole moments $\{q_l^m\}$ of the triangle Σ in coordinate system S'' .

Since for a needle-like triangle the values of ϕ_1 or ϕ_2 can be very close to $\pi/2$ which causes the base case integrals (26) to diverge. This can however be easily avoided if the BEM mesh has been constructed with sufficient quality. The second issue is that the use of theorem (2) prevents convergence of the multipole expansion within the sphere of radius $\rho + a$ centered on \mathbf{S}_0 . This is typically unimportant, since in most cases where the multipole expansion is useful, the distance between the triangle and the expansion center ρ is usually much larger than the length of the triangle's longest side a . However this restriction can be noticeable when the expansion origin and region of interest are very close to, or on, the triangle. For example if \mathbf{S}_0 is one of the vertices opposite \mathbf{P}_0 then then minimum radius of convergence would be $\sim 2a$, whereas for a numerical method which requires no translation it would only be a . Additionally, some numerical instability is expected to be encountered in the recursion relations (24) and (25) for high degree expansions where the individual terms become much larger than their difference. However, this does not appear to manifest itself until beyond $p = 32$.

7. CONCLUSION

We have presented a novel technique to evaluate the multipole expansion coefficients of a triangle. This method evaluates the necessary integrals through recursion within the context of a coordinate system with special orientation and placement. The results of the integration can then be generalized to the case of an arbitrary system through the well known transformation properties of the spherical harmonics under rotation and translation. A summary of the full method by which to compute the multipole moments of a triangle is detailed in algorithm (1).

Furthermore we have demonstrated that the application of this method to the multipole expansion of triangles with uniformly constant charge density compares favorably in terms of accuracy and speed to a simple numerical integration technique. This method can also be extended to the case of non-uniform charge density, provided the interpolant can be represented as a sum over the bivariate monomials. We expect this method may find use in solving the three dimensional Laplace equation with the fast multipole boundary element method (FMBEM). In addition, this technique has also been used for the accurate calculation of electric fields needed for large scale charged particle optics simulations. We speculate that other boundary integral equation (BIE) problems, such as the Helmholtz equation in the low frequency limit $k \rightarrow 0$, might benefit from this approach if the integrand in the multipole coefficient integrals can be expanded in terms of the solid harmonics, and may warrant a future study.

ACKNOWLEDGMENT

The authors would like to thank Dr. Ferenc Glück for valuable comments regarding the preparation of this paper. This work was performed, in part, under DOE Contract DE-FG02-06ER-41420.

APPENDIX A. INTEGRALS

The solutions to integrals of the form

$$I_p^q = \int_{\phi_1}^{\phi_2} \frac{(\sin \phi)^q}{(\cos \phi)^p} d\phi \quad (\text{A1})$$

where p and q are positive integers, can be found in any standard table of integrals [38, 39], however, for the sake of completeness we include the solutions and reduction formula here. When $p \neq q$, this integral can be simplified by the reduction relation:

$$I_p^q = \frac{-(\sin \phi)^{q-1}}{(q-p)(\cos \phi)^{p-1}} \Big|_{\phi_1}^{\phi_2} + \left(\frac{q-1}{q-p} \right) I_p^{q-2} \quad (\text{A2})$$

until the base cases I_p^0 and I_p^1 are reached. The base I_p^1 , may be solved by simple u -substitution, which yields,

$$I_p^1 = \int_{\phi_1}^{\phi_2} \frac{\sin \phi}{(\cos \phi)^p} d\phi = - \int_{\cos \phi_1}^{\cos \phi_2} \frac{du}{u^p} = \frac{u^{1-p}}{p-1} \Big|_{\cos \phi_1}^{\cos \phi_2}. \quad (\text{A3})$$

The base case of the type I_p^0 with $p > 1$ can be addressed with integration by parts, which yields the reduction relation,

$$I_p^0 = \int_{\phi_1}^{\phi_2} (\sec \phi)^p d\phi = \frac{\sin \phi (\sec \phi)^{p-1}}{(p-1)} \Big|_{\phi_1}^{\phi_2} + \left(\frac{p-2}{p-1} \right) I_{p-2}^0 \quad (\text{A4})$$

with the non-trivial base case:

$$I_1^0 = \int_{\phi_1}^{\phi_2} \sec \phi d\phi = \ln \left| \tan \left(\frac{\phi}{2} + \frac{\pi}{4} \right) \right| \Big|_{\phi_1}^{\phi_2}. \quad (\text{A5})$$

If $p = q > 1$, we simply have an integral of a power of tangent, which in turn can be reduced with

$$I_p^p = \int_{\phi_1}^{\phi_2} (\tan \phi)^p d\phi = \frac{(\tan \phi)^{p-1}}{p-1} - I_{p-2}^{p-2} \quad (\text{A6})$$

until reaching the non-trivial base case,

$$I_1^1 = -\ln |\cos \phi| \Big|_{\phi_1}^{\phi_2}. \quad (\text{A7})$$

Although most of these integrals do not have a simple closed form, the implementation of the base cases and reduction formula in computer code is a fairly simple task.

APPENDIX B. CHANGE OF INTERPOLATING BASIS

Since the evaluation of the multipole moment integral proceeds by assuming that the interpolant on the boundary element can be expressed in the basis of the bivariate monomials, in order to make these results relevant to the various interpolation methods often used (see for example, [18–21]) we need to be able to change the basis of the interpolant. Explicitly, we would like to express the interpolant as a sum over the bivariate monomials. To do this, we must determine the coefficients of the bivariate monomials in terms of the original interpolation parameters. To motivate this section, we will consider the example task of changing from the bivariate Lagrange to bivariate monomial basis. The objective we seek is to replace the tedious symbolic manipulation often encountered when performing a polynomial change of basis with a well defined numerical procedure. We expect that the results may apply to a wider class of interpolants other than Lagrange, though this extension is beyond the scope of this paper. To start, we will first introduce some basic definitions along the level of [40] or [41].

Let $R[u, v]$ be the polynomial ring over the real numbers in the variables u and v . Then for all $F(u, v) \in R[u, v]$, we may write $F(u, v)$ as the series,

$$F(u, v) = \sum_{a=0}^{n_f} \sum_{b=0}^{m_f} f_{a,b} u^a v^b \quad (\text{B1})$$

where the coefficients $f_{a,b} \in \mathbb{R}$, and $n_f, m_f \in \mathbb{N}_0$. The sum and product operations on this ring are defined in the usual sense as follows; for $F(u, v), G(u, v) \in R[u, v]$, the sum is given by:

$$F(u, v) + G(u, v) = H(u, v) = \sum_{a=0}^{n_h} \sum_{b=0}^{m_h} h_{a,b} u^a v^b \in R[u, v] \quad (\text{B2})$$

where $h_{a,b} = f_{a,b} + g_{a,b}$, and $n_h = \max(n_f, n_g)$ with m_h defined similarly. The product is given by:

$$F(u, v) \cdot G(u, v) = K(u, v) = \sum_{a=0}^{n_k} \sum_{b=0}^{m_k} k_{a,b} u^a v^b \in R[u, v] \quad (\text{B3})$$

where

$$k_{a,b} = \sum_{i=0}^a \sum_{j=0}^b f_{i,j} \cdot g_{a-i,b-j} \quad (\text{B4})$$

and $n_k = n_f + n_h$ with m_k similarly.

For a given polynomial $F(u, v)$, the greatest integer $a + b$ for which the coefficient $f_{a,b}$ is nonzero is called the maximal combined order of $F(u, v)$. We will denote the set of all bivariate polynomials $F(u, v) \in R[u, v]$ whose maximal combined order is N as P_N . In general we may write any polynomial $S^{(N)}(u, v) \in P_N$ as follows

$$S^{(N)}(u, v) = \sum_{a=0}^N \sum_{b=0}^{N-a} s_{a,b} u^a v^b. \quad (\text{B5})$$

Consider for example the first order bivariate polynomial,

$$s^{(1)}(u, v) = s_{0,0} + s_{0,1}u + s_{1,0}v. \quad (\text{B6})$$

This function can be also represented as the matrix vector product:

$$s^{(1)}(u, v) = (1, u) \underbrace{\begin{bmatrix} s_{0,0} & s_{0,1} \\ s_{1,0} & 0 \end{bmatrix}}_{R^{(1)}} \begin{pmatrix} 1 \\ v \end{pmatrix}. \quad (\text{B7})$$

The ability to write the above example in this manner motivates us to find a map between P_N and the set of $(N + 1) \times (N + 1)$ upper left triangular matrices, T_N . In general, we expect that the bivariate polynomial $S^{(N)}(u, v) \in P_N$, may be written in terms of a matrix vector product involving an upper left triangular matrix $R^{(N)} \in T_N$ whose entries correspond to the coefficients $s_{a,b}$ as follows:

$$s^{(N)}(u, v) = (1, u, \dots, u^N) \underbrace{\begin{bmatrix} s_{0,0} & s_{0,1} & s_{0,2} & \dots & s_{0,N} \\ s_{1,0} & s_{1,1} & \dots & s_{1,(N-1)} & 0 \\ s_{2,0} & \dots & s_{2,(N-2)} & 0 & \vdots \\ \vdots & \ddots & 0 & \ddots & 0 \\ s_{N,0} & 0 & \dots & 0 & 0 \end{bmatrix}}_{R^{(N)}} \begin{pmatrix} 1 \\ v \\ \vdots \\ v^N \end{pmatrix}. \quad (\text{B8})$$

Clearly, the set T_N forms a group under matrix addition, and this corresponds to the fact that P_N is also closed under addition. Unfortunately, P_N is not closed under the operation of polynomial multiplication (\cdot) , because repeated multiplication can produce a polynomial of arbitrarily large order. In order to construct a proper ring from the set P_N we must restore the property of closure by replacing the traditional product operator (\cdot) , with a new operator (\odot) which we will define as multiplication combined with the truncation of terms with combined order larger than N . Formally, for any two polynomials $F(u, v), G(u, v) \in P_N$, this operator is given by:

$$F(u, v) \odot G(u, v) = H(u, v) = \sum_{a=0}^N \sum_{b=0}^{N-a} h_{a,b} u^a v^b \in P_N \quad (\text{B9})$$

where,

$$h_{a,b} = \sum_{i=0}^a \sum_{j=0}^b f_{i,j} \cdot g_{a-i,b-j}. \quad (\text{B10})$$

We note that the (\odot) product defined in Equation (B9) only differs from the definition of normal polynomial multiplication in Equation (B3) by the limits on the summation. This definition leads us to the following lemma.

Lemma 1 *The set P_N together with the binary operations $+$ and \odot forms a ring.*

In light of lemma (1) we would also like to find a binary operator on two matrices $A, B \in T_N$ which mirrors the action of multiplication on the set P_N of bivariate polynomials. It is clear from inspection of Equations (B3) and (B4) that multiplication (\cdot) over the polynomials in $R[u, v]$ corresponds with the two dimensional convolution $(*)$ of the two matrices formed from the monomial coefficients. However, the set T_N is also not closed under the convolution operator $(*)$. To restore this closure we will instead consider a different operator \circledast , specified in definition (1).

Definition 1 *Let the two matrices A and B be elements of T_N , then the action of the binary operator \circledast on A and B produces another matrix $C \in T_N$, whose elements are given by:*

$$C_{a,b} = \begin{cases} \sum_{i=0}^a \sum_{j=0}^b A_{i,j} B_{a-i,b-j} & a + b \leq N \\ 0 & a + b > N \end{cases} \quad (\text{B11})$$

Choosing the \circledast operator to be defined as the product operation over T_N produces the following lemma.

Lemma 2 *The set T_N together with the binary operations of matrix addition $+$ and the operator \otimes forms a ring.*

To make use of the two rings $(P_N, +, \odot)$ and $(T_N, +, \otimes)$ in the problem of determining the monomial coefficients of an interpolant, we now need a bijective map between the two which preserves the structure of the operations on each ring. Specifically, we need an isomorphism, $\Lambda : (P_N, +, \odot) \rightarrow T_N(P_N, +, \otimes)$. Equation (B8) has already demonstrated the nature of $\Lambda^{-1} : (T_N, +, \otimes) \rightarrow (P_N, +, \odot)$ as a matrix vector product, and leads us to definitions (2) and (3), and theorem (3).

Definition 2 *Since we may write all $F(u, v) \in P_N$ according to Equation (B5), we define the map $\Lambda : P_N \rightarrow T_N$ as $\Lambda(F(u, v)) = R$, where the entries of the matrix $R \in T_N$ are given in terms of the monomial coefficients of $F(u, v)$ by $R_{i,j} = f_{i,j}$ and are zero when $N < i + j$.*

Definition 3 *For all $R \in T_N$, we define the map $\Lambda^{-1} : T_N \rightarrow P_N$ as follows,*

$$\Lambda^{-1}(R) = F(u, v) \tag{B12}$$

where the bivariate polynomial $F(u, v) \in P_N$ is given by the following matrix vector product,

$$F(u, v) = \mathbf{u}^T R \mathbf{v} \tag{B13}$$

and where the column vectors \mathbf{u} and \mathbf{v} of length $N + 1$, have their i -th entry given (as powers of the variables u and v) by u^i and v^i respectively.

Theorem 3 *The inverse of the map $\Lambda : P_N \rightarrow T_N$, is given by $\Lambda^{-1} : T_N \rightarrow P_N$, moreover the map Λ is a isomorphism from the ring $(P_N, +, \odot)$ to the ring $(T_N, +, \otimes)$.*

Now that we are in a position to make use of the isomorphism Λ , we will also make some assumptions on the class interpolants upon which we wish to make the change of basis. The first assumption is that interpolant $\Pi_N(u, v)$ of maximal combined order N may be written in terms of a finite set of basis polynomials $\Phi_N \subset P_N$ as,

$$\Pi_N(u, v) = \sum_j U_j p_j^{(N)}(u, v) \tag{B14}$$

where $p_j^{(N)}(u, v) \in \Phi_N$ and the U_j are know as the interpolation coefficients. The second assumption is that any higher order basis function of the interpolant can be expressed as linear combination of products of the first order basis functions. We will term such a class of interpolants as *simple* according to definition (4).

Definition 4 *Assume that a given class of two dimensional interpolating polynomials has the set of first order basis functions given by*

$$\Phi_1 = \{p_0^{(1)}, p_1^{(1)}, \dots, p_m^{(1)}\} \subset P_1. \tag{B15}$$

Now consider all multi-sets C_i of size $1 \leq k \leq N$, formed by making all possible combinations (with repetition allowed) from elements of Φ_1 . The number of multi-sets C_i is given by:

$$M = \sum_{k=1}^N \binom{m+k}{k}. \tag{B16}$$

If the class of interpolants is such that any N -th order basis polynomial $p_j^{(N)}$ can be written as,

$$p_j^{(N)} = \sum_{i=0}^{M-1} \gamma_{i,j} \prod_{x \in C_i} x \tag{B17}$$

where $\gamma_{i,j} \in \mathbb{R}$ and C_i is the i -th multi-set of size $k \leq N$, and which for all $x \in C_i$, we have $x \in \Phi_1$, then we will call such a class *simple*. We will call the set of coefficients $\gamma_{i,j}$ together with the corresponding set of multi-sets C_i , the rule of this simple class.

With this definition in mind, we can now approach the problem of converting from a bivariate Lagrange basis to a bivariate monomial basis. Specifically, we wish to find the bivariate monomial coefficients of the polynomial N -th order Lagrange interpolant $\Pi_N(u, v)$. Computationally, this amounts to finding the entries of the matrix $\Lambda(\Pi_N(u, v)) = R^{(N)}$ given the set of interpolation coefficients $\{U_j\}$.

We will follow the notation of [18, 19], who define the first order Lagrange interpolant for a triangle composed of vertices $\mathbf{P}_j = (u_j, v_j)$ as:

$$\Pi_1(u, v) = \sum_{j=0}^2 U_j p_j^{(1)}(u, v) \quad (\text{B18})$$

where,

$$p_j^{(1)}(u, v) = \frac{1}{2A}(\tau_{kl} + \eta_{kl}u - \xi_{kl}v) \quad (\text{B19})$$

and

$$\tau_{kl} = u_k v_l - v_k u_l \quad (\text{B20})$$

$$\xi_{kl} = u_k - u_l \quad (\text{B21})$$

$$\eta_{kl} = v_k - v_l \quad (\text{B22})$$

while (j, k, l) is any cyclic permutation of $(0, 1, 2)$. The area of the triangle is denoted by A . Within the context of the coordinate system S , we have $\mathbf{P}_0 = (0, 0)$, and $u_1 = u_2 = h$, so we may directly write down the basis functions $p_j^{(1)}$ as:

$$p_0^{(1)}(u, v) = \frac{1}{2A} [(v_1 - v_2)(u - h)] \quad (\text{B23})$$

$$p_1^{(1)}(u, v) = \frac{1}{2A} [v_2 u - h v] \quad (\text{B24})$$

$$p_2^{(1)}(u, v) = \frac{1}{2A} [-v_1 u + h v] \quad (\text{B25})$$

which have the corresponding coefficient matrices of:

$$R_0^{(1)} = \frac{1}{2A} \begin{bmatrix} h(v_2 - v_1) & (v_1 - v_2) \\ 0 & 0 \end{bmatrix} \quad (\text{B26})$$

$$R_1^{(1)} = \frac{1}{2A} \begin{bmatrix} 0 & v_2 \\ -h & 0 \end{bmatrix} \quad (\text{B27})$$

$$R_2^{(1)} = \frac{1}{2A} \begin{bmatrix} 0 & -v_1 \\ h & 0 \end{bmatrix}. \quad (\text{B28})$$

To obtain the bivariate monomial coefficients $\pi_{a,b}$ of the polynomial $\Pi_1(x, y)$ it is then only a simple matter of summing each matrix weighted with the appropriate Lagrange interpolation coefficient.

$$\pi_{a,b} = \left[\sum_{j=0}^2 U_j R_j^{(1)} \right]_{a,b} \quad (\text{B29})$$

In order to extend this to N -th order interpolation we could again compute the coefficients $\pi_{a,b}$ explicitly through direct inspection of the N -th order basis polynomials. However, for higher orders this quickly becomes tedious even with the use of a computer algebra system. Alternatively we can make use of the isomorphism Λ between the rings $(P_N, +, \odot)$ and $(T_N, +, \otimes)$. We note that since the bivariate Lagrange basis is a *simple* class of interpolating polynomials, we can express any N -th order basis functions according to Equation (B17) as:

$$\Pi_N(u, v) = \sum_{j=0}^{(N+1)(N+2)/2-1} U_j p_j^{(N)}(u, v). \quad (\text{B30})$$

Furthermore, under the isomorphism Λ the *rule* of the N -th order Lagrange basis can be re-expressed in the space of T_N by:

$$R_j^{(N)} = \sum_{i=0}^{M-1} \gamma_{ij} \prod_{x \in C_i} \otimes \Lambda(x) \tag{B31}$$

where we use $\prod \otimes$ to denote a repeated product of the \otimes operator over the matrices given by $\Lambda(x)$. This allows us to compute coefficient matrices $R_j^{(N)}$ directly from the first order coefficient matrices $R_j^{(1)}$ solely through matrix summation and the use of the \otimes operator. Then, to compute the bivariate monomial coefficients $\pi_{a,b}$ we only need to perform the sum:

$$\pi_{a,b} = \left[\sum_{j=0}^{(N+1)(N+2)/2-1} U_j R_j^{(N)} \right]_{a,b} . \tag{B32}$$

As an example, consider the second order Lagrange interpolant, given by,

$$\Pi_2(u, v) = \sum_{j=0}^5 U_j p_j^{(2)}(u, v) \tag{B33}$$

with the *rule* of the second order basis functions defined by:

$$p_j^{(2)}(u, v) = p_j^{(1)} \left(2p_j^{(1)} - 1 \right) = 2 \left(p_j^{(1)} \right)^2 - p_j^{(1)} \quad : \quad 0 \leq j < 3 \tag{B34}$$

$$p_j^{(2)}(u, v) = 4p_\epsilon^{(1)} p_\delta^{(1)} \quad : \quad 3 \leq j < 6 \tag{B35}$$

where $\epsilon = j \bmod 3$, and $\delta = (j + 1) \bmod 3$. Using Equation (B31) to re-express equations (B34) and (B35) in terms of coefficient matrices, $R_j^{(2)}$, yields:

$$R_j^{(2)} = 2 \left(R_j^{(1)} \otimes R_j^{(1)} \right) - R_j^{(1)} \quad : \quad 0 \leq j < 3 \tag{B36}$$

$$R_j^{(2)} = 4R_\epsilon^{(1)} \otimes R_\delta^{(1)} \quad : \quad 3 \leq j < 6. \tag{B37}$$

Thus the bivariate monomial coefficients of the polynomial $\Pi_2(u, v)$ can be computed in terms of the interpolation coefficients U_j and coefficient matrices $R_j^{(2)}$ of the second order basis functions by:

$$\pi_{a,b} = \left[\sum_{j=0}^5 U_j R_j^{(2)} \right]_{a,b} . \tag{B38}$$

Algorithm 2 Compute bivariate monomial coefficients of a simple interpolant.

Input: Triangle $\Sigma : \{\mathbf{P}_0, \mathbf{P}_1, \mathbf{P}_2\}$ and set of coefficients $\{U_j\}$ of the N -th order *simple* interpolant $S^{(N)}(u, v)$ with *rule* $(\{\gamma_{i,j}\}, \{C_i\})$.

- 1: Compute coordinate system S for triangle Σ according to Equation (9).
- 2: Compute (u, v) coordinates of $\{\mathbf{P}_0, \mathbf{P}_1, \mathbf{P}_2\}$ in S .
- 3: Form the matrices $R_j^{(1)}$ of the coefficients of the 1st order polynomials in the bivariate monomial basis according to Equations (B26), (B27), and (B28).
- 4: Compute the coefficient matrices $R_j^{(N)}$ of the N -th order basis polynomials according to Equation (B31) and the *rule* $(\{\gamma_{i,j}\}, \{C_i\})$.
- 5: Sum the coefficient matrices $R_j^{(1)}$ weighted by their interpolation coefficient U_j according to Equation (B32) to obtain the matrix M .
- 6: Map each element of M to the bivariate monomials coefficient $s_{a,b}$ of $S^{(N)}(u, v)$ according to the isomorphism $\Lambda^{-1} : T_N \rightarrow P_N$.

Output: The set of bivariate monomials coefficients $\{s_{a,b}\}$ of $S^{(N)}(u, v)$.

In a similar fashion, this method can be applied to any class of *simple* interpolants, summarized in algorithm (2).

REFERENCES

1. Poljak, D. and C. A. Brebbia, *Boundary Element Methods for Electrical Engineers*, Vol. 4, WIT Press, 2005.
2. Szilagy, M., *Electron and Ion Optics*, Springer, 1988.
3. Liu, Y., *Fast Multipole Boundary Element Method: Theory and Applications in Engineering*, Cambridge University Press, 2009.
4. Lazić, P., H. Štefančić, and H. Abraham, “The robin hood method — A new view on differential equations,” *Engineering Analysis with Boundary Elements*, Vol. 32, No. 1, 76–89, 2008.
5. Formaggio, J. A., P. Lazić, T. J. Corona, H. Štefančić, H. Abraham, and F. Glück, “Solving for micro-and macro-scale electrostatic configurations using the robin hood algorithm,” *Progress In Electromagnetics Research B*, Vol. 39, 1–37, 2012.
6. Rokhlin, V., “Rapid solution of integral equations of classical potential theory,” *Journal of Computational Physics*, Vol. 60, No. 2, 187–207, 1985.
7. Greengard, L. and V. Rokhlin, “The rapid evaluation of potential fields in three dimensions,” *Vortex Methods*, 121–141, 1988.
8. Beatson, R. and L. Greengard, “A short course on fast multipole methods,” *Wavelets, Multilevel Methods and Elliptic PDEs*, 1–37, Oxford University Press, 1997.
9. Epton, M. A. and B. Dembart, “Multipole translation theory for the three-dimensional laplace and Helmholtz equations,” *SIAM Journal on Scientific Computing*, Vol. 16, No. 4, 865–897, 1995.
10. Van Gelderen, M., “The shift operators and translations of spherical harmonics,” *DEOS Progress Letters*, Vol. 98, 57, 1998.
11. Jackson, J. D., *Classical Electrodynamics*, Wiley, 3rd Edition, 1998.
12. Lether, F. G., “Computation of double integrals over a triangle,” *Journal of Computational and Applied Mathematics*, Vol. 2, No. 3, 219–224, 1976.
13. Mousa, M.-H., R. Chaine, S. Akkouche, and E. Galin, “Toward an efficient triangle-based spherical harmonics representation of 3D objects,” *Computer Aided Geometric Design*, Vol. 25, No. 8, 561–575, 2008.
14. Proriol, J., “Sur une famille de polynomes á deux variables orthogonaux dans un triangle,” *CR Acad. Sci. Paris*, Vol. 245, 2459–2461, 1957.
15. Dubiner, M., “Spectral methods on triangles and other domains,” *Journal of Scientific Computing*, Vol. 6, No. 4, 345–390, 1991.
16. Owens, R., “Spectral approximations on the triangle,” *Proceedings of the Royal Society of London. Series A: Mathematical, Physical and Engineering Sciences*, Vol. 454, No. 1971, 857–872, 1998.
17. Koornwinder, T., “Two-variable analogues of the classical orthogonal polynomials,” *Theory and Application of Special Functions (Proc. Advanced Sem., Math. Res. Center, University Wisconsin, Madison, Wis., 1975)*, 435–495, Academic Press New York, 1975.
18. Wait, R. and A. Mitchell, *Finite Element Analysis and Applications*, Books on Demand, 1985.
19. Taylor, R. L., “On completeness of shape functions for finite element analysis,” *International Journal for Numerical Methods in Engineering*, Vol. 4, No. 1, 17–22, 1972.
20. Barnhill, R. E. and J. A. Gregory, “Polynomial interpolation to boundary data on triangles,” *Mathematics of Computation*, Vol. 29, No. 131, 726–735, 1975.
21. Chen, G. and J. Zhou, *Boundary Element Methods*, Computational Mathematics and Applications, Academic Press, 1992.
22. Gander, W., “Change of basis in polynomial interpolation,” *Numerical Linear Algebra with Applications*, Vol. 12, No. 8, 769–778, 2005.
23. Abramowitz, M. and I. A. Stegun, *Handbook of Mathematical Functions: With Formulas, Graphs, and Mathematical Tables*, Courier Dover Publications, 1966.

24. Mason, J. C. and D. C. Handscomb, *Chebyshev Polynomials*, Chapman & Hall/CRC, 2002.
25. Pinchon, D. and P. E. Hoggan, "Rotation matrices for real spherical harmonics: General rotations of atomic orbitals in space-fixed axes," *Journal of Physics A: Mathematical and Theoretical*, Vol. 40, No. 7, 1597, 2007.
26. Gimbutas, Z. and L. Greengard, "A fast and stable method for rotating spherical harmonic expansions," *Journal of Computational Physics*, Vol. 228, No. 16, 5621–5627, 2009.
27. Wigner, E. and J. J. Griffin, *Group Theory and Its Application to the Quantum Mechanics of Atomic Spectra*, Academic Press, New York, 1959.
28. Edmonds, A. R., *Angular Momentum in Quantum Mechanics*, Princeton University Press, 1958.
29. Choi, C. H., J. Ivanic, M. S. Gordon, and K. Ruedenberg, "Rapid and stable determination of rotation matrices between spherical harmonics by direct recursion," *The Journal of Chemical Physics*, Vol. 111, No. 19, 8825–8831, 1999.
30. Lessig, C., T. De Witt, and E. Fiume, "Efficient and accurate rotation of finite spherical harmonics expansions," *Journal of Computational Physics*, Vol. 231, No. 2, 243–250, 2012.
31. White, C. A. and M. Head-Gordon, "Rotating around the quartic angular momentum barrier in fast multipole method calculations," *The Journal of Chemical Physics*, Vol. 105, 5061, 1996.
32. Berntsen, J., T. O. Espelid, and A. Genz, "An adaptive algorithm for the approximate calculation of multiple integrals," *ACM Transactions on Mathematical Software*, Vol. 17, 437–451, Dec. 1991.
33. Cowper, G., "Gaussian quadrature formulas for triangles," *International Journal for Numerical Methods in Engineering*, Vol. 7, No. 3, 405–408, 1973.
34. Duffy, M. G., "Quadrature over a pyramid or cube of integrands with a singularity at a vertex," *SIAM Journal on Numerical Analysis*, Vol. 19, No. 6, 1260–1262, 1982.
35. Golub, G. H. and J. H. Welsch, "Calculation of gauss quadrature rules," *Mathematics of Computation*, Vol. 23, No. 106, 221–230, 1969.
36. Saad, Y. and M. H. Schultz, "GMRES: A generalized minimal residual algorithm for solving nonsymmetric linear systems," *SIAM Journal on Scientific and Statistical Computing*, Vol. 7, No. 3, 856–869, 1986.
37. Read, F., "Improved extrapolation technique in the boundary element method to find the capacitances of the unit square and cube," *Journal of Computational Physics*, Vol. 133, No. 1, 1–5, 1997.
38. Hudson, R. G. and J. Lipka, *A Table of Integrals*, John Wiley & Sons, 1917.
39. Peirce, B. O., *A Short Table of Integrals*, Ginn & Company, 1910.
40. Papantonopoulou, A., *Algebra: Pure & Applied*, Prentice Hall, 2002.
41. Beachy, J. A. and W. D. Blair, *Abstract Algebra*, Waveland Press, 2006.